Analysis and Experimental Validation of Various Photovoltaic System Models

Olivier Gergaud, Bernard Multon, Hamid Ben Ahmed

7th International ELECTRIMACS Congress, Montréal, august 2002.

Analysis and Experimental Validation of Various Photovoltaic System Models

O. GERGAUD, B. MULTON, H. BEN AHMED
LESiR - Brittany Branch, ENS de Cachan - Ker Lann Campus - 35170 Bruz - FRANCE
Phone: (33) 2 99 05 52 64 - Fax: (33) 2 99 05 93 28
e-mail: Gergaud@bretagne.ens-cachan.fr

Abstract -- **A photovoltaic conversion chain is classically composed of flow-through photovoltaic panels, by means of a converter, on a continuous voltage bus bar. In the present case, it has also been fitted with instrumentation for measuring weather conditions. In this article, we propose the modeling set-up for such a chain, in the aim of estimating its energy production. In order to characterize the photovoltaic panels, we have applied and compared the models available in the literature. The characteristic of converters equipped with an MPPT (Maximum Power Point Tracking) function is determined on the basis of experimental readings. All meteorological data recorded by the system are then averaged; we have also analyzed the impact of averaging frequency on the energy output of the derived model.**

Index Terms -- *P***hotovoltaic power system, modeling, power and energy analysis.**

I. Introduction

The work performed herein has contributed to generating the full-scale model of a joint photovoltaic and wind production system (20 ASE modules for a total of 2 kW peaks and 2 wind turbines running at 750 W each) hooked up to the network via a continuous bus bar and associated with an electrochemical storage device (48 V - 15 kWh) [1,5]. The ultimate objective is to derive a model that proves both accurate enough to distinguish energy transfers and fast enough to enable optimizing the sizing and/or handling of the system's energy transfers.

This article focuses on the photovoltaic conversion chain, in the aim of providing an estimation of energy production.

The photovoltaic conversion chain consists of the following :

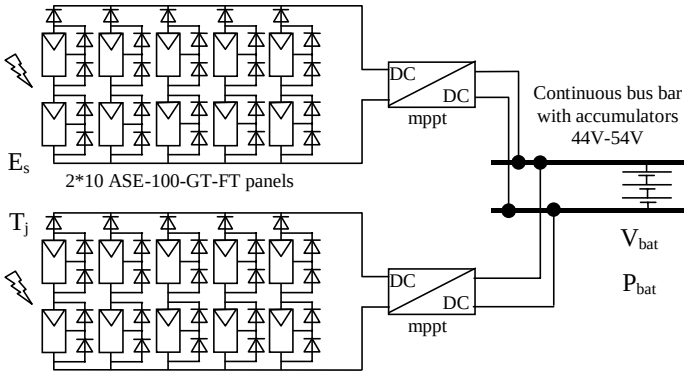

Fig. 1: Photovoltaic conversion chain

The objective of this set-up is to obtain the power characteristic being supplied to the continuous bus bar, P_{bat}, as a function of both the meteorological and electrical conditions, i.e. the insolation in the plane of solar panels E_s, their temperature T_j, along with the voltage level of the continuous bus bar, V_{bat}.

During an initial stage, we will determine the power characteristics of each panel group. We have implemented and compared various models found in the literature. Using experimental recordings, we will then ascertain the characteristic of the MPPT-tracked DC-DC converters (MSTE MPT 1000K).

II Electrical Models of the Panels

We are seeking to determine the maximum power that each group of panels is capable of supplying for a given insolation and temperature. We have applied and compared the three following models in terms of ease of use, computation time and accuracy.

A The "one-diode model"

This model is the most classical one found in the literature [6,7] and involves: a current generator for modeling the incident luminous flux, a single diode for the cell polarization phenomena, and two resistors (series and shunt) for the losses. The model of an individual cell has been diagrammed in the following figure:

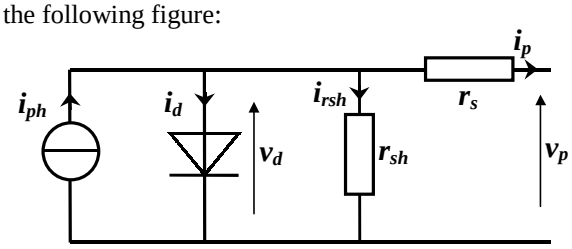

Fig. 2: Equivalent electrical diagram of a cell (1-diode model)

Each panel group consists of a series/parallel association of n_s*n_p elementary cells, with n_s denoting the number of cells in branched series and n_p the number of parallel branches. The photovoltaic generator shown below is thereby obtained.

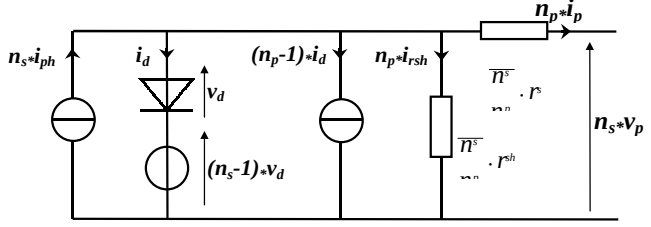

Fig. 3: Equivalent electrical diagram of a panel group (1-diode model)

In the subsequent discussion, the following notations will be employed:

$$I_{ph} = n_s.i_{ph} \; ; \; I_G = n_p.i_p \; ; \; I_d = n_s.i_d \; ; \; I_{rsh} = n_p.i_{rsh} \quad (1)$$

$$V_d = ns.v_d \; ; \; V_G = n_s.v_p \; ; \; R_s = (n_s/n_p).r_s \text{ and } R_{sh} = (n_s/n_p).r_{sh} \quad (2)$$

This model contains a total of four variables; the two input variables are:

- E_s : insolation in the panel plane (W/m²);
- T_j : junction temperature of the panels (°C).

The two output variables are:

- I_G : current supplied by the panel group (A);
- V_G : voltage level at the panel group terminals (V).

The characteristic equation for panel group PV, as deduced from the equivalent electrical diagram in Figure 2, can then be derived:

$$I_G = I_{ph} - I_d - I_{rsh} \quad (3)$$

The photocurrent, I_{ph}, is directly dependent upon both insolation and panel temperature, and may be written in the following form:

$$I_{ph} = P_1 \cdot E_s \cdot [1 + P_2 \cdot (E_s - E_{ref}) + P_3 \cdot (T_j - T_{jref})] \quad (4)$$

E_{ref} corresponds to the reference insolation of 1000 W/m² and T_{jref} to the reference panel temperature of 25°C. P_1, P_2 and P_3 are constant parameters.

The polarization current of junction PN, denoted I_d, is given by the expression:

$$I_d = I_{sat} \cdot [exp (\frac{q}{k \cdot A \cdot n_s \cdot T_j} (V_G + Rs \cdot I_G)) - 1] \quad (5)$$

where:

- I_{sat} : saturation current,
- k : Boltzmann's constant ($1{,}38.10^{-23}$ J/K),
- q : elementary charge ($1{,}6.10^{-19}$ C),
- A : ideality factor of the junction.

The saturation current is written as follows:

$$I_{sat} = P_4 \cdot T_j^3 \cdot exp (-\frac{E_g}{k \cdot T_j}) \quad (6)$$

where E_g represents the gap energy and P_4 is a constant parameter.

Lastly, the shunt current is:

$$I_{sh} = \frac{V_p}{R_{sh}} \quad (7)$$

The final equation of the model can thereby be expressed by:

$$I_G = P_1 \, . \, E_s \, . \, [1 + P_2 \, . \, (E_s - E_{ref}) + P_3 \, . \, (T_j - T_{jref})] - \frac{V_G}{R_{sh}}$$

$$- n_p \, . \, P_4 \, . \, T_j^3 \, . \, exp(-\frac{E_g}{k \cdot T_j}) \, . \, [exp(\frac{q}{k \cdot A \cdot n_s \cdot T_j} (V_G + R_s \cdot I_G)) - 1] \quad (8)$$

It should be pointed out that an implicit function of the following form is thus obtained:

$$I_G = f(I_G, V_G, E_s, T_j) \quad (9)$$

with a total of 7 parameters (P_1, P_2, P_3, P_4, A, R_s and R_{sh}) to be determined.

B The "two-diode model"

According to this model set-up, two diodes are present for the PN junction polarization phenomena. These diodes represent the recombination of the minority carriers, which are located both at the surface of the material and within the volume of the material. In this particular case, the photovoltaic generator becomes the one depicted below:

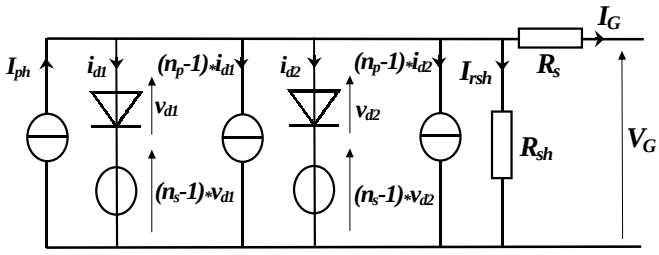

Fig. 4: Equivalent electrical diagram of a panel group (two-diode model)

The following equation is then obtained:

$$I_G = I_{ph} - I_{d1} - I_{d2} - I_{rsh} \quad (10)$$

with I_{ph} and I_{sh} maintaining the same expressions as above. For the recombination currents:

$$I_{d1} = I_{sat1} \, . \, [exp (\frac{q}{k \cdot A \cdot n_s \cdot T_j} (V_G + R_s \cdot I_G)) - 1] \quad (11)$$

$$I_{d2} = I_{sat2} \, . \, [exp (\frac{q}{2 \cdot k \cdot A \cdot n_s \cdot T_j} (V_G + R_s \cdot I_G)) - 1] \quad (12)$$

The saturation currents then become:

$$I_{sat1} = P_4 \cdot T_j^3 \cdot exp (-\frac{E_g}{k \cdot T_j}) \quad (13)$$

$$I_{sat2} = P_5 \cdot T_j^3 \cdot exp (-\frac{E_g}{2 \cdot k \cdot T_j}) \quad (14)$$

The final equation of the model is thereby written as:

$$I_G = P_1 \, . \, E_s \, . \, [1 + P_2 \, . \, (E_s - E_{ref}) + P_3 \, . \, (T_j - T_{jref})] - \frac{V_G}{R_{sh}}$$

$$-n_p.P_4.T_j^3.exp (-\frac{E_g}{k \cdot T_j}) \cdot [exp(\frac{q}{k \cdot A \cdot n_s \cdot T_j} (V_G + R_s \cdot I_G)) - 1]$$

$$-n_p.P_5.T_j^3.exp(-\frac{E_g}{2 \cdot k \cdot T_j}).[exp(\frac{q}{2 \cdot k \cdot A \cdot n_s \cdot T_j} (V_G + R_s \cdot I_G)) - 1] \quad (15)$$

with a total of 8 parameters (P_1, P_2, P_3, P_4, P_5, A, R_s and R_{sh}) to be determined.

C The "polynomial model"

The two previous models have enabled us to determine the voltage/current characteristic of the two panel groups for a given insolation and panel temperature. From this basis, it then becomes possible to determine the maximum power capable of being supplied by the panel groups under a set of given weather conditions.

The manufacturer's documentation indicates the following characteristic for maximum power P_{G_MAX}:

$$P_{G\_MAX} = P_1 \,.\, E_s \,.\, (1 + P_2 \,.\, (T_j - T_{jref})) \quad (16)$$

With P_1 lying in the range of 0.95-1.05 (0.095 to 0.105 for a single panel), and P_2 = -0.47%.

We were able to observe, from an empirical standpoint, that by adding a parameter (P_3) to the manufacturer's characteristic, results prove to be considerably improved:

$$P_{G\_MAX} = P_1 \cdot [1 + P_2 \,.\, (T_j - T_{jref})] \cdot (P_3 + E_s) \quad (17)$$

This simplified model has made it possible to ascertain the maximum power supplied by a panel group for a given insolation and panel temperature with just 3 constant parameters to be determined (P_1, P_2 and P_3) and a simple equation to be solved.

III Determination of parameter values - Power analysis

The identification of parameter values has been carried out by means of a binary genetic algorithm (GA) using experimental measurements recorded at our test site (see Table 1).

As regards the actual characteristics applied, we sought to include several measurements that span a wide insolation variation range. In the discussion below, the index i of the various magnitudes will correspond with the insolation and temperature characteristics laid out in the following table:

TABLE 1
Insolation and temperature indices of the cells used for parameter identification

Group 1		
Index i	Insolation in the panel plane (W/m²)	Cell temperature (°C)
1	100	10.8
2	127	11.5
3	189	13.9
4	260	16.5
5	399	22.6
6	494	25.3
7	592	27.9
8	704	29.6
9	854	50

For the first two models presented, the identification process was performed using the actual PV power/voltage characteristics (P^i_{actual}, $V^i_{Gactual}$). We noticed in the second part that the final equation translating the action of a group of photovoltaic panels was in fact an implicit function of the form : $I_G = f(I_G,V_G,E_s,T_j)$. The solution to the equation $I^i_{Gtheoretic} = f(I^i_{Gtheoretic}, V^i_{Gactual}, E^i_s, T^i_j)$ therefore enables us to compute the error F_i committed by the model on the power/voltage characteristic corresponding with the insolation and temperature of index "i":

$$F^i = \frac{\left| P^i_{actual} - (V^i_{Gactual} \cdot I^i_{Gtheoretic}) \right|}{P^i_{actual}} \quad (18)$$

Parameter identification was conducted for several insolation-temperature couples. The function to be minimized by the GA is thus the sum of the errors committed for each couple. Since the objective herein is to obtain the maximum power supplied by the panels, we included a weighting factor in the F^i error calculations so as to provide greater weight in the vicinity of P_{G_MAX}.

It should be pointed out that the solution to the implicit function for the $I^i_{Gtheoretic}$ calculation entails substantial computation time. Moreover, the use of GA techniques for identifying parameter values compels us to repeat this calculation many times. For this reason and in an effort to limit computation time, $I^i_{Gtheoretic}$ may be obtained by solving the equation: $I^i_{Gtheoretic} = f(I^i_{Gactual}, V^i_{Gactual}, E^i_s, T^i_j)$. Once the GA has converged on the proper solution, both $I^i_{Gactual}$ and $I^i_{Gtheoretic}$ are expected to display practically the same values.

As for the third model (the polynomial model), parameter values are determined from the maxima of the actual PV power/voltage characteristics.

TABLE 2
Parameter values derived with the one-diode model for each panel group

One-diode model (IS units)		
Parameter	Group 1	Group 2
P_1	$15.59\ 10^{-3}$	$15.21\ 10^{-3}$
P_2	0	$1\ 10^{-4}$
P_3	$8.70\ 10^{-4}$	$2.23\ 10^{-3}$
P_4	953.82	833.47
A	1	1
R_s	0.203	0.271
R_{sh}	106.04	85.69

TABLE 3
Parameter values derived with the two-diode model for each panel group

Two-diode model (IS units)		
Parameter	Group 1	Group 2
P_1	$15.57\ 10^{-3}$	$15.23\ 10^{-3}$
P_2	0	$-1\ 10^{-4}$
P_3	$1.29\ 10^{-3}$	$2.17\ 10^{-3}$
P_4	647.69	646.97
P_5	$2.44\ 10^{-3}$	$1.16\ 10^{-3}$
A	1	1
R_s	0.256	0.289
R_{sh}	118.54	89.04

TABLE 4
Parameter values derived with the polynomial model for each panel group

Polynomial model (IS units)		
Parameter	Group 1	Group 2
P_1	0.98	0.99
P_2	$-2.91\ 10^{-3}$	$-4.7\ 10^{-3}$
P_3	40.83	45

Figure 5 below reveals the power/voltage characteristics obtained using the one-diode model along with the

experimental measurements corresponding to the case of panel group 1.

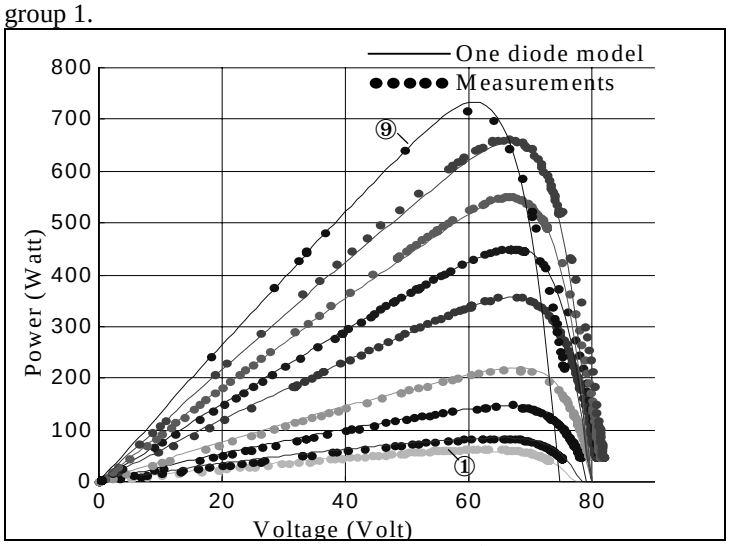

Fig. 5: Power/voltage characteristics, comparison of measurements with the GROUP 1 "one-diode model"

For the third model (polynomial), the optimization step was solely carried out on maximum power values; the following figure shows the maximum measured power as a function of the maximum power computed by this model.

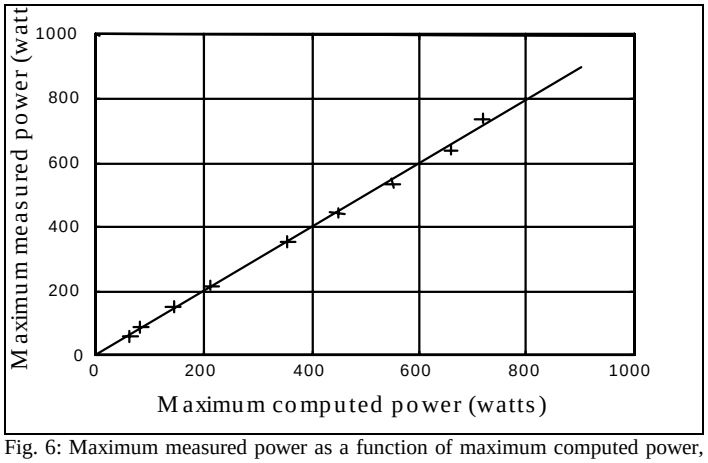

Fig. 6: Maximum measured power as a function of maximum computed power, comparison of measurements with the GROUP 1 "polynomial model"

TABLE 5

COMPARISON OF ERRORS ON THE MAXIMUM POWER VALUE OBTAINED WITH EACH MODEL - GROUP 1

Error (in %) of GROUP 1 maximum power			
Index	1-diode	2-diode	Polynomial
1	7.73	8.34	-4.35
2	-0.72	1.65	4.21
3	0.64	4.05	3.33
4	-1.75	1.85	1.86
5	3.82	2.92	-0.94
6	1.26	2.96	-1.57
7	0.92	3.78	-2.72
8	0.78	3.49	-3.22

In the ensuing discussion, we will focus exclusively on the maximum power supplied by the panels, i.e. what we are assuming to correspond to perfect MPPT control. As a means of comparing the effectiveness of the various models, we have collated in the following set of tables the model errors committed on the maximum power values for each experimental measurement. Since the readings with an index of "9" do not contain a sufficient number of points, they have not been included in these tables.

It is not possible to draw any conclusions on the quality of the models strictly from an analysis of Table 5. We now propose conducting an energy analysis of the models previously discussed.

IV ENERGY ANALYSIS

For the purposes of this analysis, we have taken measurements during the normal operations of both the panels and their MPPT-tracked converters: converter input power (i.e. panel output power), insolation and temperature. In assuming that converters are equipped with a perfect MPPT-tracked system, the power measured would then be the maximum power the panels are capable of supplying for the insolation and temperature recorded at the particular point in time.

On the following figures as a means of example, the values obtained from recordings conducted on December 17, 2001 can be observed, along with the results yielded by the two-diode model.

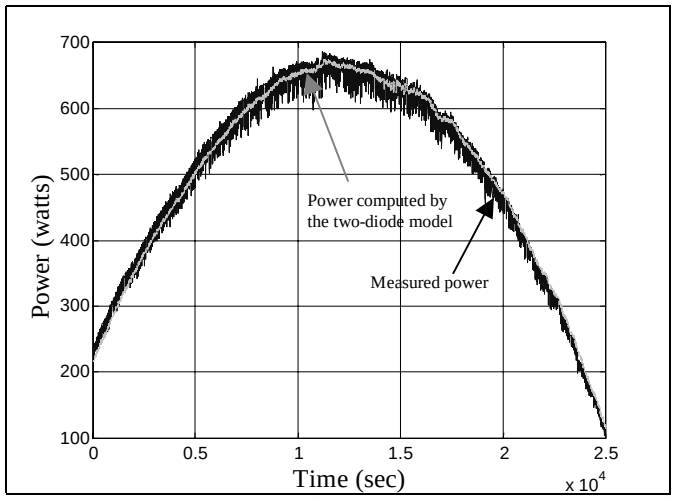

Fig. 7: Power characteristics as a function of voltage time, comparison of measurements with the GROUP 1 "two-diode model" over a one-day production period (Dec. 17, 2001)

The results listed in the following table were derived for the energy produced during this recording campaign, with a 25-second averaging time:

TABLE 6

ENERGY PRODUCED DURING THE DECEMBER 27, 2001 RECORDING CAMPAIGN BY PANEL GROUP 1: MEASUREMENT/MODEL COMPARISON

	Energy	Error
Measurement	3.493 kWh	
1-diode	3.575 kWh	+82 Wh (2.3%)
2-diode	3.467 kWh	-26 Wh (-0.9%)
Polynomial	3.478 kWh	-15 Wh (-0.4%)

We then performed the same analysis for the second panel group and obtained the following results:

TABLE 7
ENERGY PRODUCED DURING THE DECEMBER 27, 2001 RECORDING CAMPAIGN BY PANEL GROUP 2: MEASUREMENT/MODEL COMPARISON

	Energy	Error
Measurement	3.480 kWh	
1-diode	3.518 kWh	+38 Wh (+1.1%)
2-diode	3.502 kWh	+22 Wh (+0.6%)
Polynomial	3.527 kWh	+47 Wh (+1.4%)

As the tables clearly indicate, these comparisons were drawn for a day with undisturbed insolation (absence of cloud cover). We also performed the same comparison with the January 24, 2002 recordings, for a day with substantial cloud cover. Figure 8 depicts the results obtained using the polynomial model:

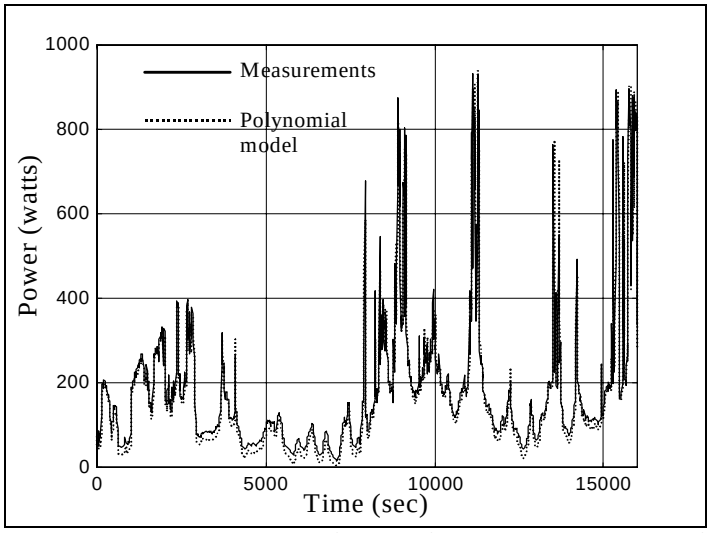

Fig. 8: Power characteristics as a function of voltage time, comparison of measurements with the GROUP 1 "one-diode model"

Tables 8 and 9 present the values of energy produced during these recordings, with a 25-second averaging time:

TABLE 8
ENERGY PRODUCED DURING THE DECEMBER 27, 2001 RECORDING CAMPAIGN BY PANEL GROUP 1: MEASUREMENT/MODEL COMPARISON

	Energy	Error
Measurement	812 Wh	
1-diode	767 Wh	-45 Wh (-5.5%)
2-diode	744 Wh	-68 Wh (-8.4%)
Polynomial	762 Wh	-50 Wh (-6.15%)

TABLE 9
ENERGY PRODUCED DURING THE DECEMBER 27, 2001 RECORDING CAMPAIGN BY PANEL GROUP 2: MEASUREMENT/MODEL COMPARISON

	Energy	Error
Measurement	806 Wh	
1-diode	753 Wh	-53 Wh (-6.6%)
2-diode	751 Wh	-55 Wh (-6.8%)
Polynomial	761 Wh	-45 Wh (+5.6%)

Thanks to the preceding recordings, we can state that these models perform well for insolation levels above the 100 watts per square meter range and just slightly less well, yet still satisfactory, outside this range.

V CHARACTERISTICS OF THE MPPT CONVERTERS

In order to determine the output of the MPPT-tracked converters, we have conducted a large number of recordings of both the MPPT input and output power characteristics and then averaged these data to generate a uniform distribution over the entire power range.

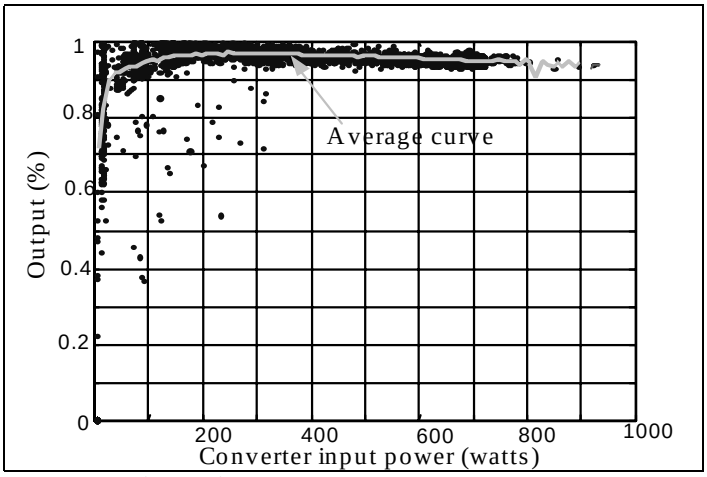

Fig. 9: Cloud of points for converter output and the corresponding average curve

For the output, we have assumed that the losses could be represented by the following expression:

$$P_{losses} = P_0 + K_1 . P_s^2 + K_2 . P_s \quad (18)$$

where:
- P_s : converter output power,
- P_0 : empty converter losses,
- K_1 : a coefficient representing the losses proportional to the square of the current, and
- K_2 : losses proportional to the current.

As such, output can be written in the form:

$$\eta = \frac{1}{1 + \frac{P_0}{P_s} + K_1 \cdot P_s + K_2} \quad (19)$$

with P_0, K_1 and K_2 being the three unknown parameters.

The first parameter, P_0, can be determined from measurement of the power consumed by the converter when insolation is zero (i.e. during nighttime hours). We have

derived the same value for both converters to be: P_0 = 1.4 W. The manufacturer's documentation indicates a value of P_0<1.44W.

It should be noted that P_0 depends to a great extent on battery voltage; given the low levels of losses however, we will not take account of this dependence. The two other parameters, K_1 and K_2, were determined so as to best approximate the average output curves. The final results are thereby:

TABLE 10
PARAMETERS OBTAINED FOR THE TWO-CONVERTER MODEL

Parameter	Group 1	Group 2
P_0	1.4	1.4
K_1	$4.14\ 10^{-5}$	$6.524\ 10^{-5}$
K_2	$19.843\ 10^{-3}$	$20.307\ 10^{-3}$

VI COMPLETE SYSTEM

In the previous sections, we first modeled the panels and then the converters. We will now proceed with an energy analysis of our models for the complete (PV + MPPT converter) system over a several-day period. These measurements were taken between March 30 and April 4, 2002 at our test site.

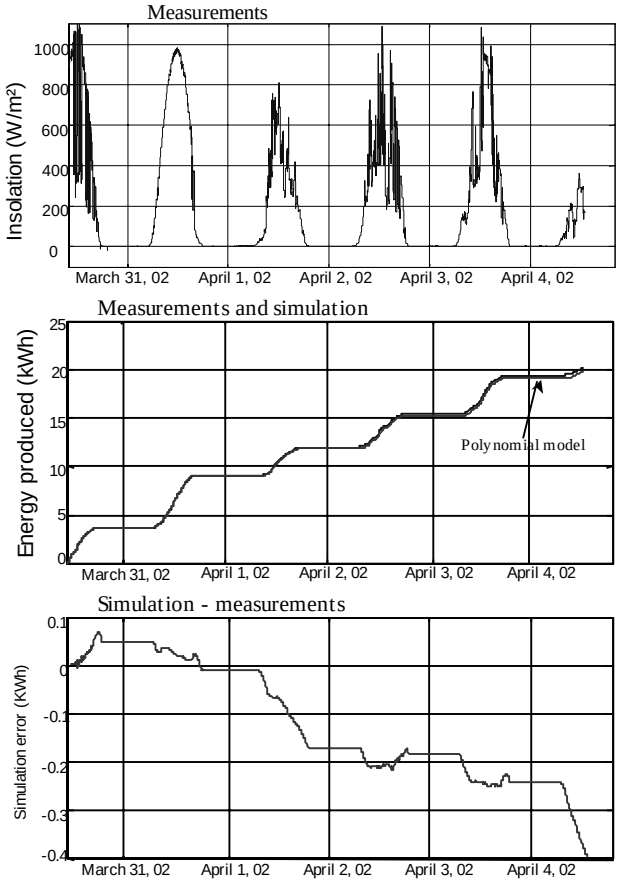

Fig. 10: Measured insolation, measurements and simulation of the energy produced for panel group 2 using the polynomial model, and simulation error on the energy produced

The simulation presented above corresponds to panel group 2 with the polynomial model. It can be observed that towards the end of the simulation, simulation error on the energy produced reaches 400 Wh, i.e. a level of barely -2%.

The results obtained with the other models and for panel group 1 are presented in the following table:

TABLE 11
ERRORS ON THE ENERGY PRODUCED DURING THE MARCH 30-APRIL 4, 2002 RECORDING CAMPAIGN: MEASUREMENT/MODEL COMPARISON

	One-diode model	Two-diode model	Polynomial model
Group 1	+0.61%	-2.09%	-0.93%
Group 2	+0.77%	+0.2%	-1.98%

It is clear that in terms of energy precision, the three models presented herein all yield highly satisfactory results. Since the errors identified lie below the 2% level, they may just as easily stem from insolation, temperature and power production measurements or from the fact that we assumed the MPPT-tracked system for converters to be perfect as they may from our models.

The meteorological recordings used as the basis for our analysis have been averaged. We have assessed the impact of averaging frequency on the energy output of our models. This assessment was conducted for averaging periods ranging between 30 seconds and 1 hour; the length of the averaging period did not exert an impact on energy output since the maximum power relationship as a function of insolation remains quite linear.

VII CONCLUSION

The work discussed herein was performed in the aim of developing an energy-based model of the photovoltaic conversion chain of a low-power photovoltaic and wind production system. For purposes of simulating the complete system, we need models that enable generating reliable energy output within sufficiently limited computation times.

We have presented and compared two models from the literature, as well as a model built from the manufacturer's documentation and measurement readings from our test site. While none of the models studied displayed a distinctively higher level of energy precision, the polynomial model did stand out for its simulation speed: for the same computation, both the one- and two-diode models took several minutes to yield their results whereas the polynomial model only required in the hundreds of milliseconds.

The polynomial model has therefore been selected for subsequent use in modeling the photovoltaic chain as part of our system optimization efforts.

VIII REFERENCES

[1] W.D. KELLOGG *et al.*, "Generation Unit Sizing and Cost Analysis for Stand-Alone Wind, Photovoltaic and Hybrid Wind/PV Systems", IEEE Trans. Energy Conv., Vol. 13, No. 1, March 1998, pp. 70-75.

[2] B.S. BORWY and Z.M. SALAMEH, "Methodology for Optimally Sizing the Combination of a Battery Bank and PV Array in a Wind/PV Hybrid System", IEEE Trans. Energy Conv., Vol. 11, No. 2, June 1996, pp. 367-375.

[3] F. GIRAUD and Z.M. SALAMEH, "Steady-state Performance of a Grid Connected Rooftop Hybrid Wind-Photovoltaic Power System with Battery Storage", IEEE Trans. Energy Conv., Vol. 16, No. 1, March 2001, pp. 1-7.

[4] R. CHEDID and S. RAHMAN, "Unit Sizing and Control of Hybrid Wind-Solar Power Systems", IEEE Trans. Energy Conv., Vol. 12, No. 1, March 1997, pp. 79-85.

[5] O. GERGAUD, B. MULTON and H. BEN AHMED, "Modélisation d'une chaîne de conversion éolienne de petite puissance", Electrotechnique du Futur 2001, Nov. 2001, Nancy, France, pp. 17-22.

[6] L. PROTIN and S. ASTIER, "Convertisseurs photovoltaïques", Techniques de l'ingénieur Génie Electrique, D3 360.

[7] V. QUASCHNING, "Numerical simulation of current-voltage characteristics of photovoltaic systems with shaded solar cells", Solar Energy, Vol. 56, No. 6, pp. 513-520, 1996.